

A Comparative Study of Star Formation Efficiencies in Nearby Molecular Cloud Complexes

Yasuo Fukui and Akira Mizuno
Department of Astrophysics
Nagoya University

Abstract We present new observational data of ^{13}CO J=1-0 emission in nearby molecular cloud complexes in Taurus, Ophiuchus, and Orion, and compare star formation efficiencies in the three regions. The ^{13}CO data have been obtained with the 4m millimeter telescope at Nagoya equipped with a SIS receiver having receiver temperature of 23 K in double side band. The molecular distribution is often characterized by highly filamentary, continuous distribution, rather than well defined clumps. Active star formation is taking place almost exclusively in the densest regions in the molecular distributions. The filamentary distributions often show velocity gradients perpendicular to their elongation, suggesting that they are spinning around their major axes. Roles of photoionization and the spinning motion on formation of stars and clouds are discussed as a step toward understanding the mechanism regulating star formation efficiencies.

1. Introduction

Stars are being formed in molecular clouds. Nearby molecular clouds allow detailed observations at various wavelengths with little contamination by background objects, and are, thereby, most suitable to study star formation in molecular clouds. The present millimeter observations of molecular clouds are far from complete because of limited spatial coverage in high angular resolution studies, or because of limited angular resolution in large scale surveys. This is particularly true for nearby dark cloud complexes subtending huge angular extents, like Taurus and Ophiuchus. It is of vital importance to have complete knowledge on molecular distributions of a few arc min resolution in these regions in order to better understand low mass star formation.

We have been carrying out a systematic survey of star formation regions within 1 kpc of the sun in the CO J=1-0 emission with the 4 m millimeter telescope at Nagoya University. The principal aim of the survey is to obtain an unbiased view of molecular distributions in these regions. The ^{12}CO emission is powerful to probe outflow phenomenon from recently formed stars, whereas the ^{13}CO emission, or the C^{18}O emission in regions with highest molecular column densities, serves as a tracer of molecular cloud cores. The beam size of this survey, $\sim 3'$, is suitable for detecting these key observational features of star formation in nearby cloud complexes. The ^{12}CO survey has resulted a discovery of 52 outflows, corresponding to about a third of the CO

outflows known at present (Fukui et al. 1986, Fukui 1989, Fukui et al. 1990a), and have revealed an evolutionary trend of molecular outflows indicating that molecular outflow corresponds to the main accretion phase of a solar type protostar (Fukui et al. 1989). The collaborators in this project are H. Ogawa, K. Kawabata, T. Iwata, K. Sugitani, S. Nozawa, J. Yang, Y. Minoshima, Y. Teshima, H. Dobashi, K. Imaoka, and T. Nagahama.

In this paper, we shall present new ^{13}CO data of three nearby molecular complexes in Taurus, Ophiuchus, and Orion, use them in order to derive star formation efficiencies ($=M_{\text{star}}/M_{\text{cloud}}$), and discuss their astrophysical implications.

2. Observations

Most of the molecular observations presented in this paper were made in ^{13}CO J=1-0 emission with the 4m telescope at Nagoya University equipped with a 4 K cooled niobium superconducting mixer receiver having a receiver temperature of 23 K at 110 GHz in double side band (Ogawa et al. 1990). The velocity resolution provided by an acousto-optical spectrometer was 0.1 km s^{-1} , sufficiently high for probing detailed velocity distributions in regions of low mass star formation. Most of the observations were carried out from December 1989 to May 1990, and 50000 ^{13}CO spectra with typical rms noise level of 0.2 K in 0.1 km s^{-1} resolution have been obtained in Taurus, Ophiuchus, and Orion (the Orion south giant molecular cloud including L1641). Areas of 50 square degrees were fully sampled every 2' with a 3' beam. The ^{13}CO data were used to calculate LTE molecular masses with an assumed $^{13}\text{CO}/\text{H}_2$ ratio of 2×10^{-6} . H_2 column density is converted to A_v by the following equation; $N(\text{H}_2) = 1.25 \times 10^{21} A_v \text{ (cm}^{-2}\text{)}$.

3. Taurus ($d = 140 \text{ pc}$)

A fully sampled ^{13}CO map of the Taurus complex, consisting of 20000 spectra, is shown as a false color map in Figure 1. In addition to several molecular condensations, filamentary distributions of molecular gas are clearly seen with a general trend of elongation nearly along the galactic plane with a tilt angle of $\sim 20^\circ$. In Figure 2, individual clouds are identified such as Heiles cloud 2 (HCL2) including TMC1, B213, L1495, B18 including TMC2, and L1536. Two major condensations, HCL2 and L1495, have molecular masses of $\sim 800 M_\odot$, respectively, and the total molecular mass of the clouds shown in Figure 1 is $\sim 3000 M_\odot$. One of the most remarkable features of the ^{13}CO distribution is the filamentary cloud toward B213. This filament, characterized by an unusually large line width of 3 km s^{-1} , is associated with another filament that is extending normal to the B213 filament to the north at $1 \sim 170^\circ$ (Figure 1). There is no OB association in Taurus.

A series of channel maps of ^{13}CO intensity are shown in Figure 3, illustrating the highly filamentary nature of the ^{13}CO distribution even more clearly. A general trend obvious in Figure 3 is that HCL2 and L1495 are linked by several filamentary clouds, showing a large scale velocity gradient in the sense that the east part is blue shifted relative to the west part. A detailed account of the data will be published elsewhere (Mizuno et al. 1990b, in preparation).

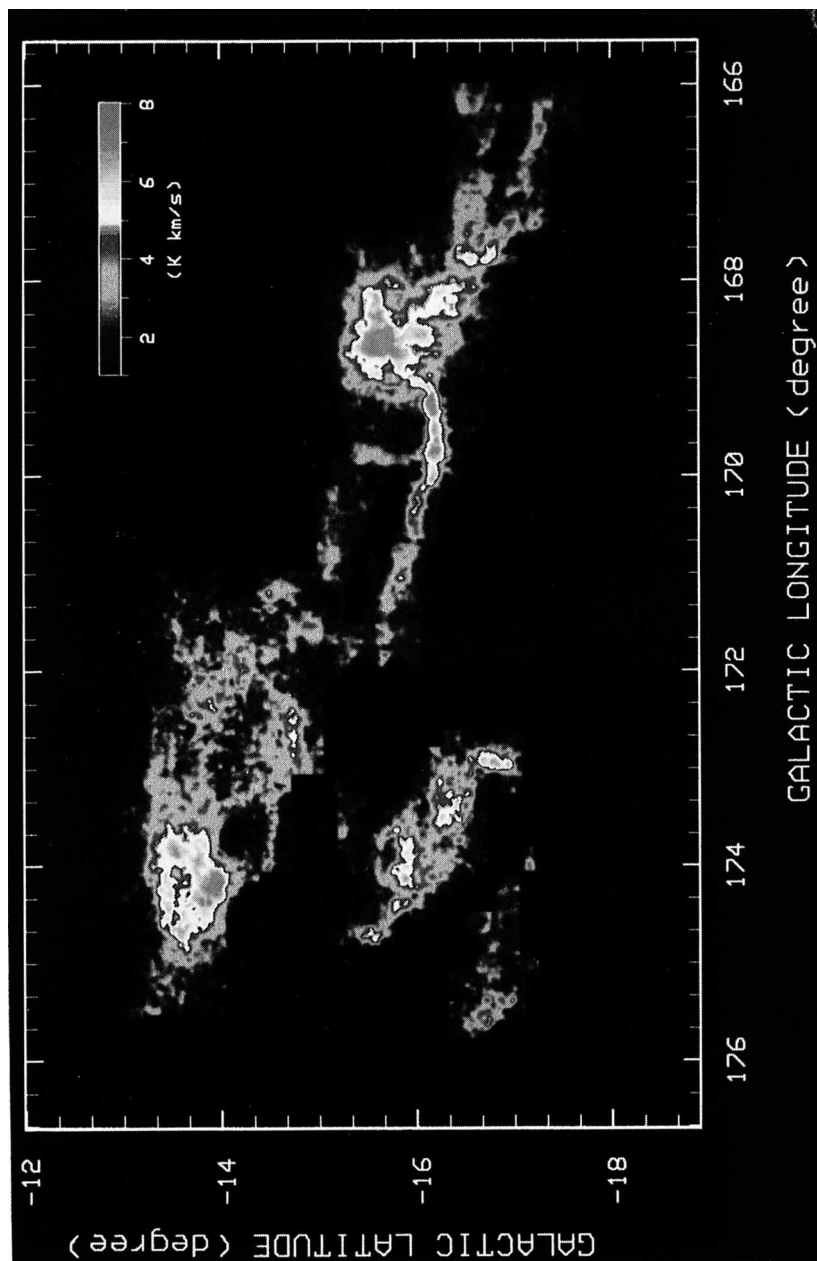


Figure 1 False-color image of total intensity in ^{13}CO (J=1-0) in the Taurus region.
(See *Color-plates section*)

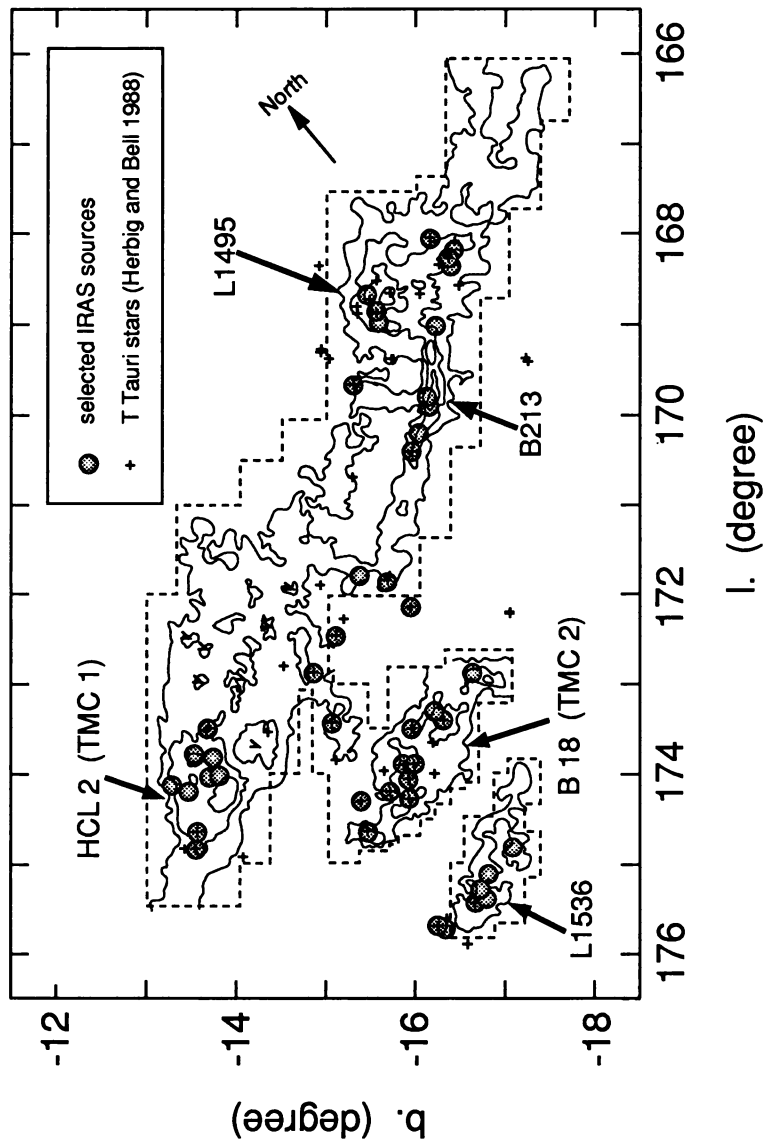


Figure 2 The selected IRAS sources and T Tauri stars (Herbig and Bell 1988) are superposed on the ^{13}CO ($J=1-0$) total intensity contour map. Contours are every 2K km s^{-1} from 2K km s^{-1} in T_A^* . The boundaries of the observed area are denoted by dashed lines. The selection criteria for the IRAS point sources are as follows; i) significantly detected at more than two wavelengths (quality flags are 2 or 3), and ii) flux densities more than 1 Jy at either $25\text{ }\mu\text{m}$ or $60\text{ }\mu\text{m}$.

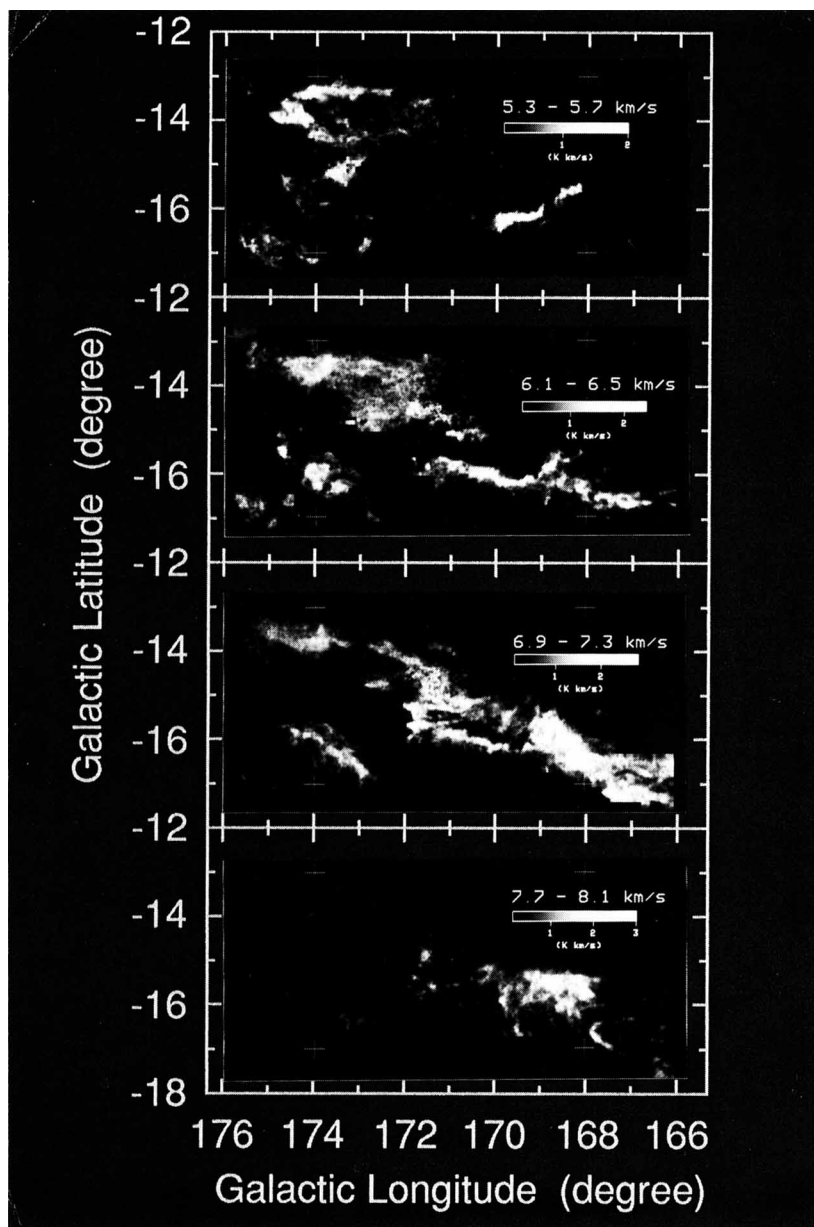


Figure 3 Grey-scale images of ^{13}CO (J=1-0) velocity channel maps in the Taurus region. The velocity intervals for the four panels are 5.3 - 5.7 km s⁻¹, 6.1 - 6.5 km s⁻¹, 6.9 - 7.3 km s⁻¹, and 7.7 - 8.1 km s⁻¹ (from top to bottom), respectively.

We used data on T Tauri stars compiled by Herbig and Bell (1988) and on IRAS point sources (IRAS Catalogs and Atlases) as indications of recent star formation. These young stellar objects are certainly highly concentrated in the densest parts of the molecular gas as indicated in Figure 2, where the lowest contour corresponds to H_2 column density of $2\text{--}3 \times 10^{21} \text{ cm}^{-2}$. Since the IRAS and ^{13}CO data sample the region almost fully, the remarkable coincidence between them strongly indicates that stars are being formed in the molecular gas having large column densities, i.e. large A_V 's. The outer parts of HCL2 and L1495, having low column densities, have no associated T Tauri stars or IRAS sources. On the other hand, L1536, showing also active star formation, has a smaller H_2 column density, and may be somewhat exceptional in the Taurus region. The luminosity range of the IRAS sources and T Tauri stars is from 0.1 to $10 L_{\odot}$, indicating that only low mass stars are formed in Taurus. Searches for CO outflows in Taurus are not yet complete, and are to be made in a more systematic manner.

4. Ophiuchus ($d = 160 \text{ pc}$)

The Ophiuchus dark cloud complex is extended in an area from $l \sim 350^{\circ}$ to 10° , and $b \sim 13^{\circ}$ to 23° . A ^{13}CO map of this region is shown in Figure 4 (Nozawa et al. 1990). In the southern edge of the complex, the ρ Oph main cloud is located at $l \sim 355^{\circ}$, and $b \sim 16^{\circ}$, consisting of two dense condensations associated with long ($\sim 10 \text{ pc}$) filamentary clouds, so called "interstellar streamers" (see also Loren, 1989a, 1989b). On the other hand, the northern half of the complex is highly clumpy, consisting of ~ 50 ^{13}CO clumps (Nozawa et al. 1990). The molecular mass of the ρ Oph main cloud is estimated to be $\sim 2500 M_{\odot}$, while that of the northern complex is $\sim 3000 M_{\odot}$. Sco OB2 association on the southwest of the complex is probably located at the same distance with the molecular complex.

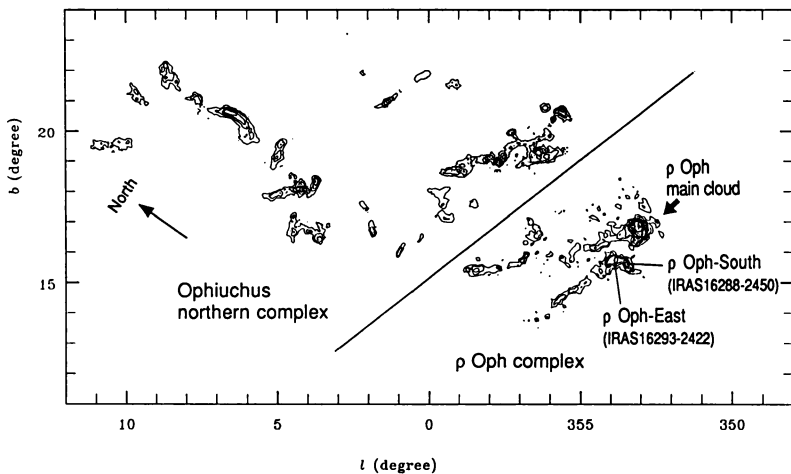


Figure 4 Total intensity map in ^{13}CO ($J=1-0$) in the Ophiuchus region. Contours in T_R^* are every 2.0 K km s^{-1} from 2.0 K km s^{-1} for the Ophiuchus northern complex and every 3.2 K km s^{-1} from 3.2 K km s^{-1} for the ρ Oph complex, respectively.

The high star formation efficiency in the ρ Oph main cloud is well recognized. Along the $C^{18}O$ ridge embedded in the main cloud, about hundred infrared sources are detected, suggesting SFE of $\geq 22\%$ (Wilking, Lada, and Young 1989). On the contrary, the neighboring secondary core is associated with only a few infrared sources, IRAS16293-2422 (ρ Oph-East outflow; Mizuno et al. 1990a), IRAS16288-2450 (ρ Oph-South outflow; Fukui 1989) etc., and even lower star formation activity is found in the two streamers. The northern part of the complex is also found to show a low level of star formation with a star formation efficiency of $\sim 0.3\%$ (Nozawa et al. 1990). The ρ Oph main cloud is therefore characterized by an unusually enhanced star formation activity in the whole Ophiuchus complex.

5. Orion ($d = 480$ pc)

The molecular cloud associated with Ori A, including L1641, is the Orion south giant molecular cloud. A new ^{13}CO map of this cloud is shown in Figure 5. This map shows several new features that are not recognized in previous ^{13}CO maps (e.g. Bally et al. 1987), particularly weak extended features around the most intense elongated ridge containing Ori KL object ($l \sim 209^\circ$). The northern half of this cloud shows sign of massive star formation as indicated by the Trapezium stars ($l \sim 209^\circ$) exciting the Orion Nebula and other luminous infrared sources. On the other hand, the luminosities of embedded infrared sources decrease toward the south, indicating that low mass stars are being formed in the southern half, consisting of the L1641 cloud, at $l \sim 211^\circ - 214^\circ$. We shall in the following focus on the L1641 cloud.

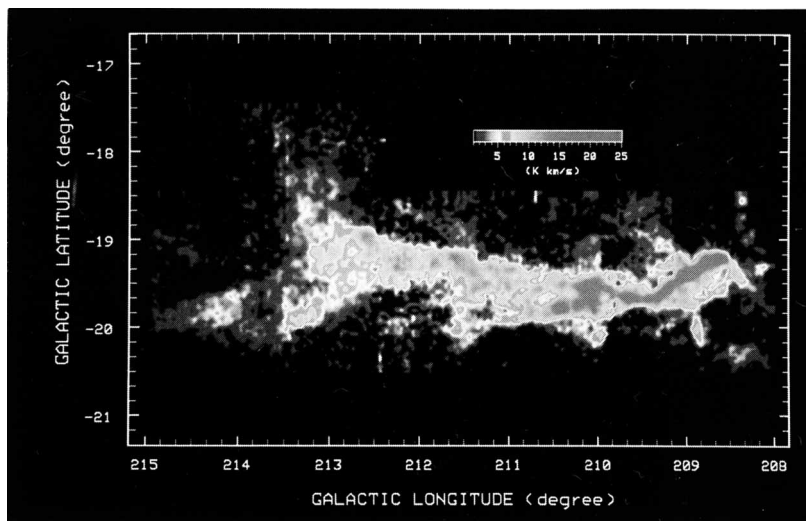


Figure 5 False-color image of the ^{13}CO ($J=1-0$) total intensity for the Orion south giant molecular cloud, involving the L1641 cloud. (See *Color-plates* section)

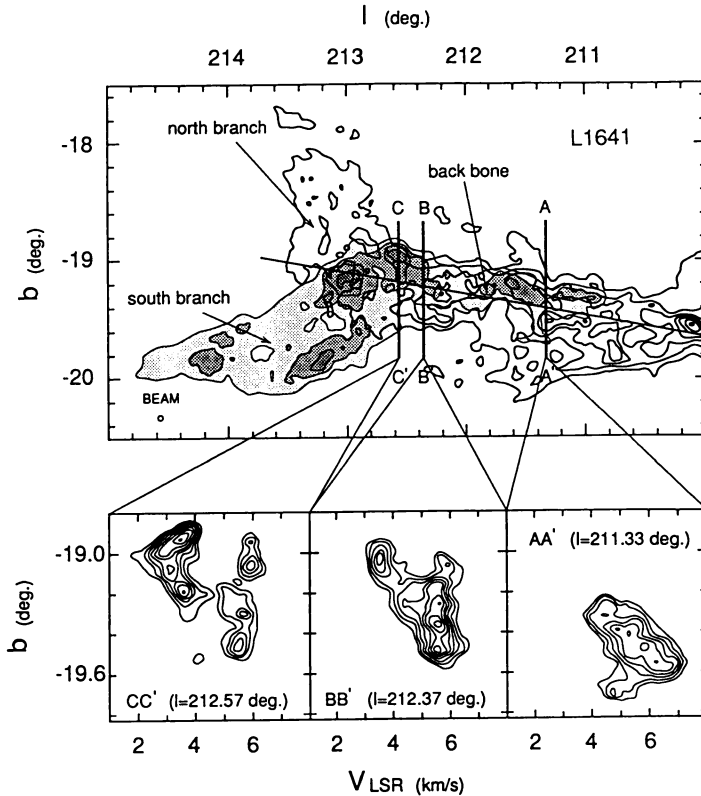


Figure 6 Distribution of the two velocity components in the L1641 cloud. In the upper panel, the ^{13}CO intensity integrated over 1 to 5 km s^{-1} and 5 to 8 km s^{-1} are shown by hatchings and contours, respectively. Contours for each are every 2 K km s^{-1} from 2 K km s^{-1} as the lowest. The lower panels show typical latitude-velocity diagrams at three longitudes. Contours of the lower panels are every 0.5 K from 2.0 K as the lowest, with velocity resolution of 0.1 km s^{-1} .

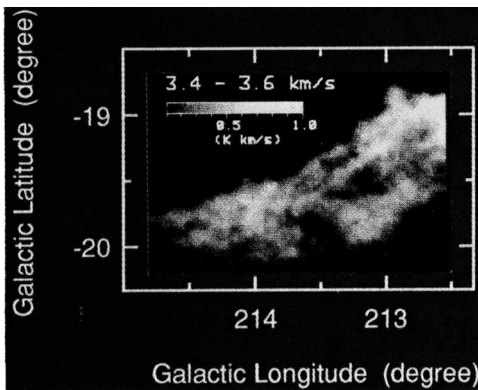


Figure 7 A grey-scale image of channel map ($v_{\text{LSR}} = 3.4$ to 3.6 km s^{-1}) for the "fish tail" part of the Orion south giant molecular cloud. The highly filamentary nature of the "fish tail" is seen.

The most interesting new result from our observations is the finding that the southern edge of the ^{13}CO cloud consists of a system of two branches of highly ordered structures. These two branches are seen as a V shape in Figure 5 at $l \sim 212^\circ.5$ to 215° and $b \sim -18^\circ$ to -20° . We shall call this V shaped structure as the "fish tail" structure from its appearance. This "fish tail" exhibits a striking velocity structure; i.e. its north and south branches show clear velocity difference (Figure 6). The south branch is blueshifted relative to the main cloud, appearing at $v_{\text{LSR}} = 2-5 \text{ km s}^{-1}$, while the north branch is redshifted at $v_{\text{LSR}} = 5-7 \text{ km s}^{-1}$. The full width of the "fish tail" in latitude is $\sim 15 \text{ pc}$ at $l \sim 213^\circ$, becoming systematically smaller in both the north and south branches to $\sim 3 \text{ pc}$ at $l \sim 212^\circ.5$. The highly filamentary nature of the "fish tail" is demonstrated in a representative channel map of a small velocity range, $v_{\text{LSR}} = 3.4 - 3.6 \text{ km s}^{-1}$, in Figure 7.

According to a ^{12}CO map obtained with the Columbia telescope, two streams of filamentary ^{12}CO emission can be traced nearly along the galactic plane down to $l \sim 216^\circ.5$ (Maddalena et al. 1986), suggesting that the "fish tail" is further extended as lower density molecular gas not detectable in the ^{13}CO emission with the current sensitivity. It is known that the molecular complex is embedded in a huge HI cloud of $10^5 M_\odot$ (Chromey, Elmegreen, and Elmegreen 1989). The masses of the north and south branches of the "fish tail" structure are $2000 M_\odot$ and $2700 M_\odot$, respectively. The total mass of the "fish tail" is then $\sim 5000 M_\odot$, about one sixths of the total mass of the main cloud between $l \sim 208^\circ$ and 213° , $\sim 30000 M_\odot$.

The L1641 cloud ($l \sim 211^\circ - 214^\circ$) is an active site of low mass star formation. Observational signatures for them are more than 50 IRAS point sources (e.g. Strom et al. 1989) and 6 molecular outflows (Fukui et al. 1989, Levereault 1988). The distribution of the IRAS sources and molecular outflows indicate that these young objects are remarkably well correlated with the ^{13}CO ridge of the L1641 cloud (Fukui et al. 1989). Most of the IRAS sources have luminosities in a range from 1 to $10 L_\odot$, consistent with that of a solar-mass star in the pre-main sequence contraction phase. Although only about one fifth of them are identified as T Tauri stars (Herbig and Bell 1988), it seems very reasonable to suppose that they are heavily obscured T Tauri stars.

6. Discussion

6.1. Star formation efficiencies

It is difficult to estimate stellar masses precisely in the early stage of star formation, since the luminosities of protostars dramatically change in time (e.g. , Shu, Adams, and Lizano 1987, Stahler, Shu, and Taam 1980). Although masses of the new-born stars are not well determined, we can estimate a frequency of star formation from the infrared and optical data. As a first order approximation of SFE, we use the number of IRAS sources and visible T Tauri stars per unit solar mass cloud. Figure 8 shows SFE's thus derived as a function of stellar bolometric luminosities in the three regions, Taurus, the ρ Oph main cloud, and L1641 in Orion. The masses of these clouds are estimated based on the present ^{13}CO ($J=1-0$) data. The databases of the stellar luminosities are the IRAS point source catalog for the IRAS sources, and, as for T Tauri stars, Herbig and Bell (1988) and Cohen, Emerson, and Beichman (1989) for Taurus, Wilking, Lada, and Young (1989) for

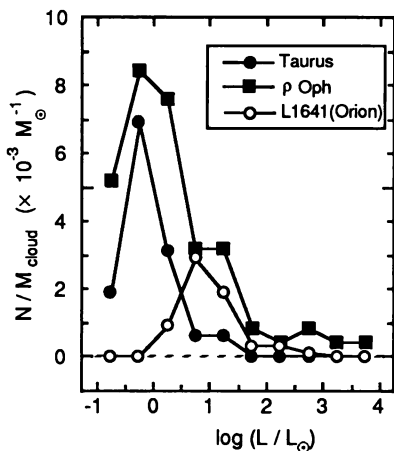


Figure 8 A plot of star formation efficiencies (S.F.E.) as a function of luminosity for Taurus, the ρ Ophiuchus main cloud, and the L1641 cloud in Orion.

ρ Oph, and Strom et al. (1989) for L1641. In Figure 8, the peak position of SFE in L1641 is by one order of magnitude larger than those in Taurus and ρ Oph. However, it is to be noted that the detection limit of IRAS data is $\sim 3 L_{\odot}$ in L1641, causing the decrease in the SFE below $3 L_{\odot}$ in L1641. The difference of peak positions does not mean that L1641 is a massive star forming region compared with Taurus and ρ Oph. Indeed, objects more luminous than $1000 L_{\odot}$ are not detected in L1641, whereas such objects are detected in ρ Oph. Above the detection limit ($\geq 3 L_{\odot}$), the number of new-born stars per unit mass in Taurus, ρ Oph, and L1641 are $\sim 1 \times 10^{-3} M_{\odot}^{-1}$, $\sim 9 \times 10^{-3} M_{\odot}^{-1}$, and $\sim 6 \times 10^{-3} M_{\odot}^{-1}$, respectively. In this luminosity range, the SFE of Taurus is much smaller than those of ρ Oph and L1641. However, in a luminosity range of $0.3 - 3 L_{\odot}$, the number of new-born stars per unit mass in Taurus, $\sim 1.2 \times 10^{-2} M_{\odot}^{-1}$, is about a half of that in ρ Oph, $\sim 2.1 \times 10^{-2} M_{\odot}^{-1}$. These results indicate that the Taurus region is an active low mass star forming region.

6.2. Ionization degree

Molecular clouds are ionized mainly by cosmic ray protons and ultraviolet radiation of OB stars. This ionization couples the molecular gas to the magnetic field, depending on the ionization degree, and results in the cloud collapse time scale an order of magnitude larger than the free fall time scale because of the magnetic pressure. This implies that star formation is effectively regulated by the degree of ionization in molecular clouds. In the deep interior of the molecular clouds, cosmic ray protons must be dominant as an ionization agent. On the other hand, near the cloud surface contribution of ultraviolet photons may be important. Photoionization therefore may well regulate star formation in molecular clouds (McKee 1989). Recent theoretical estimates have shown that ultraviolet radiation can effectively ionize molecular gas to an ionization degree of $\geq 10^{-8}$ up to A_V of ~ 4 mag from the cloud surface for a typical CO cloud having a density of 10^3 cm^{-3} (Nakano and Fukui 1990, in preparation).

The Ophiuchus northern complex is characterized by clumped distribution, favorable for penetration of radiation, has a typical A_v of ~ 7 mag, and shows a small star formation efficiency (Nozawa et al. 1990). In addition, Sco OB2 association raises the ultraviolet radiation flux by an order of magnitude above the general interstellar value. Therefore, it is probable that relatively high ionization degrees are realized in the Ophiuchus northern complex, leading to the small star formation efficiency. On the other hand, the ρ Oph main cloud, having an unusually large A_v of ~ 100 mag, must have small ionization degrees, allowing efficient ambipolar diffusion of magnetic flux and active star formation as observed.

The Taurus complex has a typical A_v of several magnitudes, implying that the general ultraviolet radiation field may be important in regulating ionization degrees. This might explain that the SFE in the densest parts of HCL2, L1495, and B18 in Taurus is significantly smaller than that in the ρ Oph main cloud. The rather large SFE in L1536 having a small A_v may need some other explanation; this cloud may have a larger gas column density previously, and may be dispersing the placental cloud material at present. This possibility could be tested by a careful analysis of the ages of the IRAS sources in L1536.

L1641 in Orion has an average A_v three times larger than that in Taurus, and active star formation is expected, if photoionization is playing a role. This is actually the case, and SFE is relatively high in L1641 (Figure 8). To summarize section 6.2, it seems that regulation of star formation by photoionization provides to a first approximation a viable explanation for the difference in star formation activity among the three regions.

6.3. Magnetic field

Optical polarization data provide information on projected direction of magnetic fields, and Zeeman measurements of atomic and molecular spectral lines may determine the field strength and orientation. The optical polarization measurements of Taurus indicate that the polarization vectors are generally normal to the molecular filaments, whereas in the ρ Oph region the optical polarization vectors are nearly parallel to the molecular filaments. Thus, there appears no simple relationship between magnetic fields and cloud elongation if the field configuration is simply assumed straight and parallel (see e.g. Goodman et al. 1990).

If the fields have a more complicated, but ordered configuration, we may find a possible solution for the problem. Such an example is found in L1641, where the optical polarization vectors are at an angle of $\sim 30^\circ$ to the major axis of the cloud, and the HI Zeeman splitting measurements indicate that the field line is reversed on the both sides of the cloud. On the basis of these data, it is suggested by Y. Uchida and J. Bally that the general magnetic field configuration is consistent with a large scale *helical* pattern (Bally 1989). This suggests that a more elaborate field configuration may be needed to explain the apparent diversity between optical polarization vectors and cloud elongation in other regions.

6.4. Origin of the filamentary distributions

The present study of three nearby molecular complexes indicates that the distribution of molecular clouds is highly filamentary. Since one of them, Taurus, is associated with no massive stars, dynamical or radiative effects of OB stars do not provide a general explanation for these filamentary distributions. Alternatively, magnetic fields may play an important role in producing the filamentary distributions, and an idea to explain formation of molecular filaments via magnetohydrodynamical mechanism is proposed by Uchida, Mizuno, Nozawa, and Fukui (1990a). We analysed the velocity field in the ρ Oph streamer, one of the most remarkable filamentary distributions, and found that the streamer shows a systematic velocity gradient of $\sim 1.5 \text{ km s}^{-1} \text{ pc}^{-1}$ across its major axis. This velocity gradient is in the same sense with the main cloud, and we interpreted that the velocity gradient indicates a spinning motion of the molecular filament accelerated by the torsional Alfvén waves emitted from the massive main cloud. This idea is essentially an interstellar version of the magnetohydrodynamical model for molecular outflow acceleration (Uchida and Shibata 1985, Pudritz and Norman 1986). Recent numerical simulations of a spinning interstellar cloud suggest that such a process really works to form filamentary clouds (Uchida, Shibata, and Rosner 1990, in preparation).

In the following, we shall show that the L1641 cloud also exhibits a remarkable spinning motion. In order to see the detailed velocity distribution, in Figure 6 are shown a series of position-velocity diagrams (b - v_{LSR} diagrams) taken at three representative longitudes near the root of the "fish tail". As shown in the cut at $l=211^{\circ}.33$, the main ridge of the L1641 cloud is characterized by a significant velocity gradient of $\sim 1 \text{ km s}^{-1} \text{ pc}^{-1}$, and this gradient is interpreted in terms of spinning motion around the major axis of the cloud by Uchida et al. (1990b). We shall call this main ridge as the "backbone" of the "fish tail". The radius of the "backbone", $\sim 1 \text{ pc}$, may be determined as a result of establishment of a nearly dynamical equilibrium state among magnetic pressure, centrifugal force, and self gravity. The magnetic field strength is then estimated to be $\sim 100 \mu\text{G}$, corresponding to an Alfvén speed of $\sim 5 \text{ km s}^{-1}$.

We suggest that the two branches of the "fish tail" represent merging filamentary structure, being wound up by the spinning main cloud. The spinning motion will pull the two branches of the "fish tail" into a twisted rope, and this merging processes the west ward extension of the "backbone". The apparent merging of the two components of the "fish tail", and their funneled shape may be well explained by such a picture. The parallel filamentary distribution of molecular gas shown in Figure 7 is a natural result of the stretching due to this twisting up. To be quantitative, the total molecular mass of the L1641 "backbone", $\sim 10000 M_{\odot}$, is large enough to dynamically influence the "fish tail" structure via magnetic tension, and the whole Orion south cloud including the Ori KL region having $\sim 30000 M_{\odot}$ may contribute in magnetically winding up the "fish tail". Thus, the total angular momentum of the main cloud is sufficient to dynamically influence the "fish tail". It is noteworthy that the helical magnetic field suggested in section 6.3 is a natural consequence of such winding up by a massive spinning cloud.

In the present picture, the coalescence, accompanying compression due to the pinching effect is causing the increase of density from $\sim 200 \text{ cm}^{-3}$ in the "fish tail" to $\sim 2000 \text{ cm}^{-3}$ in the "back bone". It is shown in section 5 that IRAS point sources, good candidates of protostars, are distributed along the "backbone" in L1641, suggesting active

low mass star formation. This star formation may be enhanced owing to the increase of molecular column density as well as the compression due to the coalescence of the two branches of the "fish tail".

The spinning picture is in a sense a very natural idea to collect matter from less dense raw material; we, human beings, have been spinning cotton into yarn since the prehistoric age. It is no wonder that the molecular clouds do the same in the interstellar space. It is however to be noted that many physical aspects remain to be clarified; the process should accompany MHD shocks, and, in some cases, reconnection of field lines. All these details are to be thoroughly investigated theoretically. It is also important to increase the number of such spinning clouds with filamentary distributions. The B213 filament in Taurus also shows a velocity gradient normal to its elongation, and a detailed analysis for it is in progress.

7. Summary

Star formation efficiencies in three nearby cloud complexes are described on the basis of new ^{13}CO data. It is shown that young stellar objects are preferentially located in the densest, heavily obscured regions in the molecular clouds. Differential photoionization may well regulate the trend in star formation efficiencies through affecting ionization degrees in molecular gas, and thereby controlling the ambipolar diffusion of the magnetic flux leading to star formation. The cloud morphology is often filamentary. Recent detailed analyses of the kinematics of these filamentary clouds suggest that the clouds are spinning along their major axes. A possible role of such spinning motion in cloud formation is discussed on the basis of the L1641 data.

We are grateful to K. Sugitani and Y. Minoshima for their invaluable help in preparing this manuscript. This research was in part financially supported by the Grant-in-Aid for Specially Promoted Research No. 01065002 in the Ministry of Education, Science, and Culture.

References

- Bally, J. 1989, in *Low Mass Star Formation and Pre-Main Sequence Objects*, ed. B. Reipurth, (European Southern Observatory, Garching bei München), p. 1.
- Bally, J., Langer, W. D., Stark, A. A., and Wilson, R. W. 1987, *Astrophys. J. Letters*, 312, L45.
- Chromey, F. R., Elmegreen, B. G., and Elmegreen, D. M. 1989, *Astron. J.*, 98, 2203.
- Cohen, M., Emerson, J. P., and Beichman, C. A. 1989, *Astrophys. J.*, 339, 455.
- Fukui, Y. 1989, in *Low Mass Star Formation and Pre-Main Sequence Objects*, ed. B. Reipurth, (European Southern Observatory, Garching bei München), p. 95.
- Fukui, Y., Iwata, T., Mizuno, A., Bally, J., and Lane, P. A. 1990a, in *Protostars and Planets III*, (in press).
- Fukui, Y., Iwata, T., Takaba, H., Mizuno, A., Ogawa, H., Kawabata, K., and Sugitani, K. 1989, *Nature*, 342, 161.
- Fukui, Y., Minoshima, Y., Uchida, Y., Mizuno, A., Iwata, T., Ogawa, H., and Takaba, H. 1990b, (submitted to *Publ. Astron. Soc. Japan*).

- Fukui, Y., Sugitani, K., Takaba, H., Iwata, T., Mizuno, A., Ogawa, H., and Kawabata, K. 1986, *Astrophys. J. (Letters)*, 311, L85.
- Goodman, A. A., Bastien, P., Myers, P. C., and Ménard, F. 1990, *Astrophys. J.*, 359, 363.
- Herbig, G. H., and Bell, K. R. 1988, University of California, Lick Observatory Bulletin No. 1111.
- IRAS Catalogs and Atlases, Explanatory Suppl. 1984, eds. C. A. Beichman, G. Neugebauer, H. J. Habing, P. E. Clegg, and T. J. Chester, (U.S. Government Printing Office, Washington D.C.).
- Leverreault, R. M. 1988, *Astrophys. J. Suppl.*, 67, 283.
- Loren, R. B. 1989a, *Astrophys. J.*, 338, 902.
- Loren, R. B. 1989b, *Astrophys. J.*, 338, 925.
- Maddalena, R. J., Morris, M., Moscowitz, J., and Thaddeus, P. 1986, *Astrophys. J.*, 303, 375.
- McKee, C. F. 1989, *Astrophys. J.*, 345, 782.
- Mizuno, A., Fukui, Y., Iwata, T., Nozawa, S., and Takano, T. 1990a, *Astrophys. J.*, 355, 184.
- Nozawa, S., Mizuno, A., Teshima, Y., Ogawa, H., and Fukui, Y. 1990, (submitted to *Astrophys. J. Suppl.*).
- Ogawa, H., Mizuno, A., Hoko, H., Ishikawa, H., and Fukui, Y. 1990, *Int. J. of Infrared and Millimeter Waves*, 11, 717.
- Pudritz, R. E., and Norman, C. A. 1986, *Astrophys. J.*, 301, 571.
- Shu, F. H., Adams, F. C., and Lizano, S. 1987, *Ann. Rev. Astron. Astrophys.*, 25, 23.
- Stahler, S. W., Shu, F. H., and Taam, R. E. 1980, *Astrophys. J.*, 241, 637.
- Strom, K. M., Newton, G., Strom, S. E., Seaman, R. L., Carrasco, L., Cruz-Gonzalez, I., Serrano, A., and Grasdalen, G. L. 1989, *Astrophys. J. Suppl.*, 71, 183.
- Uchida, Y. 1989, in *Low Mass Star Formation and Pre-Main Sequence Objects*, ed. B. Reipurth, (European Southern Observatory, Garching bei München), p. 141.
- Uchida, Y., and Shibata, K. 1985, *Publ. Astron. Soc. Japan*, 37, 515.
- Uchida, Y., Fukui, Y., Minoshima, Y., Mizuno, A., Iwata, T., and Takaba, H. 1990b, (submitted to *Nature*).
- Uchida, Y., Mizuno, A., Nozawa, S., and Fukui, Y. 1990a, *Publ. Astron. Soc. Japan*, 42, 69.
- Wilking, B. A., Lada, C. J., and Young, E. T. 1989, *Astrophys. J.*, 340, 823.